

Electron microscope comparisons of graphitic brake lining particulates, diesel exhaust particulates, and other fine and ultra-fine carbonaceous and non-carbonaceous, airborne particulates

L. E. Murr and J. J. Bang

Department of Metallurgical and Materials Engineering, and Center for Environmental Resource Management, The University of Texas at El Paso,
El Paso, TX 79968

Abstract

Particulate matter (PM) from a number of specific sources has been collected on carbon/formvar-coated 100 mesh nickel or copper grids for transmission electron microscopy (TEM) using a thermal precipitator. These sources included diesel truck exhaust, graphitic PM from brake shop environments, jet engine exhaust streams, and a wide range of general airborne PM for comparison. Individual PM TEM images were compared with corresponding selected-area electron diffraction (SAED) patterns and energy-dispersive (X-ray) spectra (EDS). Diesel PM was characterized by aggregate-branching of carbonaceous spherules while graphitic PM consisted of layered carbon and prominent mixtures of inorganic microcrystals. Essentially all airborne PM collected was characterized by variations of cluster or aggregate morphologies and non-carbonaceous PM was mostly microcrystalline or nanocrystalline. Mixtures of carbonaceous and nanocrystalline PM were also observed. Although tedious, individual PM analysis and comparison appears to be a necessary strategy to elucidate the apparent toxic effects increasingly identified with ultra-fine and nanoparticulates in the air.

Keywords: Diesel PM; Carbonaceous Particulates; Nanoparticulates; Microcrystals; Aggregates

1. Introduction

Particulate matter (PM) in the air represents a broad class of physically and chemically diverse substances. Inhalable particulates are generally defined as being equal to or less than $10\ \mu\text{m}$ in aerodynamic diameter (and designated PM 10). Recent interest has focused on so-called fine (PM 2.5) and ultra-fine or nanoparticulates (PM 0.1) which can penetrate deep into the lungs. Many fine particles (PM 2.5) are generally composed of sulfate, nitrate, organic and elemental carbon, or other carbonaceous matter, elemental or metal oxides or salts, and the like. Many components of fine particles and especially ultra-fine particulates can oscillate between the gas and aerosol phases, making their collection and measurement difficult or impossible by conventional filter-based methods. Carbonaceous PM is generally considered to be composed of two major components: organic carbon – made up of hundreds of individual carbon compounds – and elemental carbon; which can be soot, carbon black, or related carbon nanotubes or fullerenes, and graphitic matter (Shauer, et al., 1996).

Diesel particulate matter or DPM is a complex subset of fine and ultra-fine particles composed of elemental carbon, adsorbed organic compounds or carbonaceous complexes, and sometimes small amounts of sulfate, nitrate, metals, and other trace elements incorporated within or upon these complexes (EPA, 2002). These particulates are highly respirable and make excellent carriers for adsorbed inorganic and organic compounds, many of which are known to have mutagenic and carcinogenic properties (EPA, 2002). Diesel emissions (DE) as measured by DPM made up 6% of the total ambient PM 2.5 inventory in 1998 nationwide U.S. data and roughly 23% of the inventory excluding natural and miscellaneous sources (EPA, 2002). Estimates also range from 10 to 36% in some urban centers in California, Colorado, and Arizona. DE are identified with vehicle engines and non-road engines such as locomotives, marine vessels, and the like.

Graphitic particulates originating as debris from automotive friction products such as brake pads/linings, and the like, are virtually unrecorded in airborne PM assessments, and the potential for human health hazards is unknown. The use of graphite-based brake pads in the U.S. and elsewhere has become pervasive as a so-called safe alternative to asbestos products. With an estimated 40 million commercial vehicles manufactured in the U.S. alone since 1995 (Ward, 2001), the release of wear debris and the addition of graphitic PM to the atmosphere could be very significant. Furthermore, the characteristics (size, morphologies, aggregation complexities, etc.) of fine graphitic PM may promote adsorption phenomena and other features observed for DPM. The ability to distinguish graphitic PM from DPM is unproven, and more generally there are few if any efforts to distinguish carbonaceous species emitted from fossil fuel, agricultural burning, forest fires, and related sources contributing to fine, airborne PM.

It is difficult to measure individual organic compounds in the ambient air because of a variety of factors and as a consequence there have been no comparisons of various carbonaceous particulates with DPM. There are also no apparent efforts to assess airborne graphitic debris either in specific brake service environments or in the outdoor environment such as major traffic areas, etc. Correspondingly there are no comparisons of fine graphitic particulates with other carbonaceous particulates, etc.

In this research program we utilize transmission electron microscopy (TEM) and associated selected-area electron diffraction (SAED) analysis along with energy-dispersive (X-ray) spectroscopy (EDS) to characterize and compare a wide variety of fine and ultra-fine PM collected on carbon/formvar-coated TEM grids in a thermal precipitator (Murr, 1991; Bang and Murr, 2002, Bang, et al., 2003). PM characterization and comparison will include carbonaceous particulates, DPM, and graphitic brake lining debris. Standard filter/collection techniques will also be utilized in parallel with PM collection by thermal precipitation in order to establish a baseline for overall comparison and analysis.

2. Experimental Methodology

In this study we endeavored to collect, characterize, and compare diesel particulate matter (DPM), graphitic debris (PM) from brake pads and related airborne graphitic particulate matter, and airborne carbonaceous particulates. Airborne particulate matter was collected on standard 100 mesh copper or nickel transmission electron microscope (TEM) grids coated with a very thin (~35 nm) formvar film coated with an equally thin layer of evaporated carbon. These grids were placed in a thermal precipitator (TP) which has been described in detail elsewhere (Bang and Murr, 2002; Bang, et al., 2003). This device, based on simple principles of aerosol physics and thermodynamics (Hinds, 1999) has been demonstrated to have a very high efficiency for collecting fine and ultra-fine airborne particulates (Bang, et al., 2003, Hinds, 1999). The 3 mm TEM coated grid substrates are placed in an ice-water cooled copper block and the entering air stream is passed over a heated tungsten wire which produces a temperature gradient-driven adsorption characteristic to the particulates in the air stream, causing them to "stick" on the coated grid surface. These experimental grids were then placed in special sealed carrying devices until inserted into the specimen holder of the TEM. The TEM was a Hitachi H-8000 analytical electron microscope operated at 200 kV accelerating potential. It was fitted with a goniometer-tilt stage and a Noran energy dispersive (X-ray) spectrometer (EDS) system; utilizing a beryllium detector window which allows for carbon and elements above it in the periodic chart to be detected.

The TP was operated in collecting particulate matter in the vicinity of several diesel trucks and buses outdoors, in indoor brake shop locations, and at a variety of other outdoor locations around the City of El Paso, Texas, USA. Several calibration experiments were conducted utilizing cigarette or burning paper smoke, and commercially available TiO₂ nanoparticulate samples. These have been described in previous discussions of the TP design

and applications (Bang, et al., 2003). TP calibrations were also performed utilizing commercially available silver nanoparticulate matter as well.

Brake pad debris/particulate matter collected in brake shops was initially examined in a scanning electron microscope (SEM) in order to gain some overall structural perspectives. Fine particulate matter included in brake pad debris samples was observed by sprinkling on the 3 mm TEM coated grid substrates and placing a second 3 mm TEM coated grid on top to create a sandwich to contain the PM in the TEM.

Standard analysis sequences for all PM regimes in the TEM included bright-field imaging of individual particulates at convenient magnifications (50,000 to 250,000 X), obtaining a selected-area electron diffraction (SAED) pattern of the particulate, and finally obtaining an EDS spectrum of the particulate. The EDS spectrum provides relative elemental concentrations and a guide to potential compounds or mineral species listed in the X-ray card file system. The SAED pattern can provide confirming chemistry and structure by measuring the effective diffraction ring or spot radii (R) which are related to the d-spacings listed in each X-ray card file: $d\text{-spacing in } \text{\AA} = \lambda L/R$; where λL is the TEM camera constant (a fixed, calibrated value at 200 kV operation (Murr, 1991)). SAED pattern symmetries or reflection sequences can also confirm specific crystal structures and of course the pattern immediately indicates crystallinity, degree of crystallinity, polycrystallinity, crystal overlap, etc. (Murr, 1991).

3. Results and Discussion

Examples of TP Calibration and Airborne PM Collection

Figure 1 illustrates the collection efficiency of the TP utilizing a variety of fine and nanoparticulate standards which serve as an effective calibration for particulate collection. In Fig. 1(a) typical cigarette smoke particulates are observed to be characterized by a wide distribution of carbonaceous spherules ranging in aerodynamic diameter from <50 nm to $5 \mu\text{m}$. The corresponding SAED pattern and EDS spectrum are indicative of amorphous carbon, and the

sequence of analytical TEM components represented by Fig. 1(a) can serve as a baseline for carbonaceous PM.

Figure 1(b) illustrates a corresponding TEM bright-field image typical of TP collected silver nanoparticles which occur as large agglomerates or clusters of individual silver grains or single crystals ranging in size from roughly 100 nm to 500 nm. Characteristic microtwins within individual, single-crystal grains are indicated by the arrow in the TEM image in Fig. 1(b) (left). The corresponding SAED pattern is characteristic of face-centered cubic Ag ($a = 4.04\text{\AA}$), and the EDS spectrum shows Ag K(α) and L(α) spectra the Ni peaks represent the Ni 100 mesh grid which act as an elemental calibration standard as well.

Figure 1(c) shows a typical large aggregate of TiO_2 (rutile, tetragonal: $a = 4.59\text{\AA}$, $c = 2.96\text{\AA}$) crystals. Individual TiO_2 particulates are rectangular-like crystals with a minimum dimension ~ 10 nm. The corresponding TiO_2 EDS spectrum in Fig. 1(c) (right) does not contain a recognizable oxygen peak which is often the case for nano-oxide particulates because of low volume, light element signal generation. The Cu peaks in the EDS spectrum are representative of the 100 mesh Cu grid and, like Ni grids, serve as an elemental calibration.

Figure 2 shows a range of airborne particulates and particulate aggregates collected in the TP at various locations in El Paso, TX, USA. These particulate and aggregate examples represent variations in complex particulate morphologies, composition, and crystallinity. They also represent some examples of the intermixing of carbonaceous matter. For example, Fig. 2(a) illustrates a single carbonaceous particulate with a wall-like feature containing extremely fine needle crystals < 5 nm. Their corresponding diffraction spots are indicated by the arrows in the SAED pattern insert in Fig. 2(a). Figure 2(b) shows similar carbonaceous matter with no crystalline components but the carbonaceous matter consists of carbon (graphitic) layers < 10 nm thick.

Figure 2(c) shows a layer-like aggregate composed of very fine crystallites while Fig. 2(d) shows some systematically overlapped and rotated single-crystal aggregates which appear to be carbonaceous or organic in nature but which are in fact completely inorganic crystals.

Figure 2(e) shows a complex, crystalline aggregate composed of thousands of nanocrystalline particulates <1 nm in aerodynamic diameter. Such complex aggregates are common in the air and may be particularly damaging because of break-up on entering the airways and allowing the individual fragments to travel deep into the lung epithelial cells (Renwick, et al., 2001; HEI, 2001).

Figure 2(f) shows a carbonaceous particulate or complex carbonaceous cluster with no crystallinity indicated in the SAED pattern insert, only the diffuse carbon rings are evident.

Brake Shop PM Examples

Figure 3 shows, in contrast to Fig. 2, some examples of PM matter characteristic of a brake shop where graphitic brake pads were being replaced on an automobile. Figure 3(a) is a typical graphite-like, layered carbonaceous particulate with layer thicknesses of ~10 nm; similar in appearance to the random, airborne particulate shown in Fig. 2(b). However, the remainder of airborne brake shop particulate examples shown in Fig. 3 are micro or nanocrystalline aggregates of inorganic PM. In Fig. 3(b) is shown a silica (SiO_2) aggregate composed of many hundreds of individual particles and crystal fibers ≤ 10 nm. Figure 3(c) shows a sequence of TEM image, SAED pattern, and EDS spectrum for a TiO_2 (rutile) aggregate composed of 100 nm diameter crystals; with very different morphologies than those illustrated in the calibrating rutile nanocrystals shown in Fig. 1(c). Figure 3(d) shows a similar TEM image, SAED pattern (insert), and EDS spectrum for a complex cluster of copper-rich nanocrystals ranging in size from 110 nm. These large aggregates, composed of thousands of nanocrystals, pose particular respiratory tissue detriment as noted previously (Renwick, et al., 2001; HEI, 2001).

It is interesting to note that a variety of inorganic and metal-related PM accompany carbonaceous, graphitic (brake-lining related) PM. In fact graphitic brake linings are often composed of graphite intermixed with metal powders such as Fe, etc. which were not specifically collected. TiO₂, rutile, is often observed in airborne PM collections and has been observed in other city air (Katrinak, et al., 1995; Chianelli, et al., 1998). However, such observations are not necessarily unique to contemporary city air since the lungs of the Tyrolean iceman, a mummy preserved in Alpine ice for 5300 years, also contained TiO₂, crystal particulates amongst other microcrystalline PM intermixed with soot PM (Hofer, et al., 2000).

DPM Examples

Figure 4 shows several analytical sequences to collected diesel particulates (DPM). These particulates are chemically and morphologically unique in contrast to the complex variations observed for airborne PM, including graphitic PM, as shown in Fig. 2 and 3. DPM, like other carbon black and combustion soots has carbonaceous, branched shapes resulting from the interconnection of often hundreds of carbonaceous spherules (similar to those in Fig. 1(a)) which stick together through a combination of adhesive surface forces and partial coalescence occurring at high temperatures common during combustion (Fichman and Pnueli, 1985; Mountain, 1986). Figure 4(a) and (b) show typical PM collected in diesel truck exhaust streams while Fig. 4(c) and (d) illustrate PM collected in the air in a truck stop area. The SAED patterns and EDS spectra are dominated by diffuse carbon reflections and carbon peaks respectively. Traces of sulfur are often observed as indicated in the EDS spectrum of Fig. 4(d).

The individual carbonaceous spherules in the PM of Fig. 4 range in size from 10-50 nm but Fig. 4(a) illustrates a closely coalesced cluster with spherules composed of hundreds of carbon nanoparticles of ~1 nm diameter. The carbonaceous aggregates in Fig. 4(b) and (c) are composed of 300-500 branched spherules of ~50 nm average size. Like other complex, inorganic aggregates, such as those illustrated in Figs. 2(e) and 3(d), the branched DPM may

also fragment when inhaled and allow individual spherules or smaller spherule clusters (10-100 nm) to penetrate deep into the airway system.

DPM and related carbonaceous aggregates collected in urban air have been considered in the context of fractal-like morphologies which allows the branched, clustered spherules to be differentiated by fractal analysis and quantified to some extent by measuring fractal dimensions which change with combustion conditions, etc. (Katrinak, et al., 1993; Skillas, et al., 1998).

Figure 5 shows, in contrast to Fig. 4, some examples of inorganic, nanocrystalline particulate mixtures containing carbonaceous matter collected along with the characteristic, branched-clusters of carbonaceous DPM (Fig 4). The TEM, SAED pattern insert, and EDS spectrum sequence of Fig. 5(a) shows CaCl_2 intermixed with Si, Ge, and carbon. Figure 5(b) shows a TiO_2 crystal cluster similar to that collected in brake shop air as illustrated in Fig. 3(c). There is also some aluminum in the EDS spectrum along with carbon. It is especially interesting to note the similarity in crystal size and diffraction features on comparing Figs. 3(c) and 5(b). It is also interesting that TiO_2 (titania) is a characteristic PM frequently found in various, ambient air environments. Titania has been a component of paint world-wide. However, it is unknown whether this is unique to contemporary, ambient air or a universal and historical PM occurrence since, as noted earlier, crystals of titania have been observed in the lungs of a 5300 year-old mummy (Hofer, et al., 2000).

Other Combustion-Related PM Examples

Figure 6(a) illustrates wood burning-related PM characterized by clustered, branched carbonaceous spherules (~ 50 nm diameter). These aggregates are essentially pure carbon/hydrocarbon clusters very similar to DPM shown in Fig. 4.

Figure 6(b) shows a complex cluster of alumina (Al_2O_3) grains intermixed with carbonaceous matter, silica (SiO) and Cu, copper oxide or possibly copper silicate. This PM aggregate was collected in the air near a small steel mill. Figure 5(c) shows a complex copper,

silicon, aluminum polycrystalline aggregate with intermixed carbonaceous matter collected in the air proximate to a closed copper smelter. The SAED pattern insert in Fig. 6(c) is predominantly fcc copper.

High-Temperature Combustion Sources – Jet Engine Exhaust PM

Figure 7 shows several examples of aggregate carbonaceous and inorganic crystalline PM collected in the exhaust stream of small jet engines. The EDS spectrum of Fig. 6(a) indicates C, Cu, Ag and W; with W contributing significantly to the particulate composition. Figure 7(b) shows a substantial carbonaceous (carbon) peak along with some Si; the SAED pattern insert (Fig. 7(b)) shows an intermixing of very tiny silica nanocrystals.

Summary and Comparison of PM Examples

The PM examples shown in Figs. 1 to 7 illustrate that ambient air, including exhaust streams, etc., contains a wide range of particle sizes from 1 nm to $>10 >10 \mu\text{m}$; with the a propensity of these particulates actually composed of nanocrystals creating complex, crystalline aggregates or carbonaceous/nanocrystal clusters, often containing thousands of nanocrystals. Even DPM is characteristically branched, connected and interconnected carbon/carbonaceous (carbon plus hydrocarbon) spherules forming complex clusters usually containing 300 to 500 spherules. Ambient air PM therefore contains varying fractions of carbonaceous particulates and aggregates, mixtures of carbonaceous particulates and inorganic, crystalline particulates forming complex aggregates, and inorganic, crystalline aggregates often composed of thousands of nanocrystals (1-10 nm aerodynamic diameter).

Fuel combustion, especially including diesel engines and wood burning produces variations in branched, carbonaceous, spherule clusters which could be rendered less detrimental to respiratory health if the clusters could be made more dense, robust, and less prone to branch fragmentation when ingested into the airways. Generally, the smaller the particulates entering the respiratory tract the deeper their penetration into the lungs.

Consequently, ultrafine particles are considered particularly toxic (EPA, 1996; HEI Perspectives, 2002; Aust, et al., 2002). Lippmann, et al (2000) have also shown that associations between different PM size fractions and mortality, and hospital admissions, were observed for all size fractions below 10 μm , and these size fraction associations or correlations were more significant than acidity or sulfate content of PM. The effects of ultrafine particulates, regardless of chemical composition, are especially well correlated in humans and animals with pulmonary disease (Oberdörster, et al., 2000).

Although ultrafine PM is considered for comprise only 1% to 8% of ambient air PM (EPA, 1996), the fact that these particulates are complex aggregates means that their total surface areas are enormous in contrast to coarser PM, and this provides ideal conditions for photo and thermocatalytic reactions such as ozone-forming reactions (Chianelli, et al., 1998) and other complex reactions which could alter the nanocrystal surface composition. In addition, given a range of fine or ultrafine particulates of a given composition (silica), crystalline PM is more deleterious than amorphous PM (Momarca, et al., 1997).

The mechanisms of PM health effects are vague at best because the properties (size, morphology, crystallinity, chemistry, etc.) responsible for toxicity or other interference with particulate phagocytosis in the alveolar epithelium (lung tissue) are largely unknown. And since, as illustrated on comparing Figs. 2 to 7, the PM mixture is extremely complex, efforts to identify specific components of PM responsible for particular, adverse effects is very challenging. Consequently, more systematic, individual PM characterization for specific emission sources is imperative, as implicit on comparing Figs. 1 to 7: cigarette, wood, diesel, jet engine, agricultural burning, and other soot-specific PM combustion sources; and comparisons with ambient air PM, especially particulate TEM images.

4. Conclusions

Although TEM analysis of individual PM is tedious, it is essential that PM images from specific sources and PM generated by different, specific conditions be available for reference and comparison, especially in identifying complex mixtures of ambient air PM. DPM and graphitic PM from brake linings etc. are characteristically different, although brake-lining PM is also predominantly intermixed with inorganic and other metal-related, crystalline particulates. Ambient air PM is a complex mixture of carbonaceous clusters, aggregates of carbonaceous matter and inorganic crystals, and clusters and complex aggregates of inorganic crystals, (microcrystals and nanocrystals, some as small as 1 nm in diameter). Many PM aggregates are composed of thousands of nanocrystals or nanoparticles even carbon nanoparticles. DPM is especially recognizable as complex, branched clusters of hundreds of carbonaceous spherules (nominally 25 to 50 nm in diameter). High temperature combustion sources such as jet engines produce other complex aggregates. Aside from carbonaceous PM which is largely branched aggregates, ambient air PM is crystalline or mixtures of carbonaceous PM and inorganic micro or nanocrystals.

Acknowledgments

This research was supported in part by a Mr. and Mrs. MacIntosh Murchison Endowed Chair, an EPA-Southwest Center for Environmental Research and Policy (SCERP) Project A-02-3, an EPA-STAR Fellowship Award (Project U-91609601-0; J.J.B), and an EPA STAR Grant. We are especially grateful to Norma Padilla for her help in collecting brake-lining debris and particulates.

References

- Aust, A., Smith, K. R., Veranth, J. M., Hu, A., Lightly, J. S., Ball, J. C., Stracci, A. M., and Young, W. C., 2002, Particle Characteristics Responsible for Effects on Human Lung Epithelial Cells, Health Effects Institute, Boston, MA.
- Bang, J. J., and Murr, L. E., December, 2002, Collecting and Characterizing Atmospheric Nanoparticles, *JOM*, 28-30.

Bang, J. J., Trillo, E. A., and Murr, L. E., Feb., 2003, Utilization of Selected Area Electron Diffraction Patterns for Characterization of Air Submicron Particulate Matter Collected by a Thermal Precipitator, *Journal of the Air and Waste Management Association*, **53**, 1-10.

Chianelli, R. R., Yacaman, M. J., Arenas, J., and Aldape, F., 1998, Atmospheric Nanoparticles in Photocatalytic and Thermal Production of Atmospheric Pollutants, *J. Hazardous Substance Res.*, **1**, 1-1.

Environmental Protection Agency (US), 1996, Air Quality Criteria for Particulate Matter, vol. III, EPA 600/P-651001CF, National Center for Environmental Assessment, Research Triangle Park, NC.

Fichman, M., and Pnueli, D., 1985, *J. Appl. Mech.* **52**, 105-108.

Health Assessment Document for Diesel Engine Exhaust, EPA-600-8-90-057F, National Center for Environmental Assessment, Office of Research and Development, U.S. Environmental Protection Agency, Washington, D.C., May, 2002.

Health Effects Institute, 2001, Airborne Particles and Health: HEI Epidemiologic Evidence. *HEI Perspectives*, Health Effects Institute, Cambridge, MA.

HEI Perspectives, April, 2002, Understanding the Health Effects of Components of the Particulate Matter Mix: Progress and Next Steps, Health Effects Institute, Cambridge, MA.

Hinds, W. C., 1999, *Aerosol Technology: Properties, Behavior and Measurement of Airborne Particles*, 2nd Edition, (New York, Wiley & Sons, Inc.).

Hofer, F., Mitterbauer, C., Papst, I., and Pabst, M. A., 2000, EFTEM Tells Us What the Tyrolean Iceman Inhaled 5300 Years Ago, *EUREM*, **12** Brno, Czech Republic, B413-B414.

Katrinak, K. A., Anderson, J. R., and Buseck, P. R., 1995, Individual Particle Types in the Aerosol of Phoenix, Arizona, *Environ. Sci. Technol.*, **29**, 321-329.

Katrinak, K. A., Rez, P., Perkes, P. R., and Buseck, P. R., 1993, Fractal Geometry of Carbonaceous Aggregates from an Urban Aerosol, *Environ. Sci. Technol.*, **27**, 639-547.

- Lippmann, M., Ito, K., Nadas, A., and Burnett, R. T., 2000, Association of Particulate Matter Components with Daily Mortality and Morbidity in Urban Populations, Research Report 95, Health Effects Institute, Cambridge, MA.
- Momarca, S., Crebelli, R., Teretti, D., Zanardini, A., Fuselli, S., and Filini, L., 1997, Mutagens and Carcinogenesis in Size-Classified Air Particulates of a Northern Italian Town, *Sci. Total Environ.*, **205**(2-3), 137-144,
- Mountain, R. D., Mulholland, G., and Baum, G. W., 1986, *J. Colloid Interface Sci.*, **114**, 67-81.
- Murr, L. E., *Electron and Ion Microscopy and Microanalysis: Principles and Applications*, 2nd Edition, Marcel Dekker, NY, 1991.
- Oberdörster, G., Finkelstein, J. N., Johnston, C., Gelein, R., Cox, C., Baggs, R., and Elder, A.C.P., 2000, Acute Pulmonary Effects of Ultrafine Particles in Rats and Mice, Research Report 96, Health Effects Institute, Cambridge, MA.
- Renwick, L. C., Donaldson, K., and Clouter, A., 2001, Impairment of Alveolar Macrophage/Phagocytosis by ultrafine Particles, *Toxicol. Appl. Pharmacol.* **172**, 119-127.
- Shauer, J. J., Rogge, W. F., Hildemann, L. M., Mazuek, M. A., Cass, G. R., and Simoneit, B.R.T., 1996. Source Apportionment of Airborne Particulate Matter Using Organic Compounds as Tracers, *Atmospheric Environment*, **30**, 3837-3855.
- Skillas, G., Kunzel, S., Burtscher, H., Baltensperger, U., and Siegmann, K., 1998, High Fractal-Like Dimension of Diesel Soot Agglomerates, *J. Aerosol. Sci.*, **29**(4),m 411-419.
- Ward's Motor Vehicle Facts and Figures, 2001, Southfield, MI.

Figure Captions

Figure 1. Thermal precipitator collection/collection calibration (a) TEM, SAED pattern, EDS sequence corresponding to TP-collected cigarette smoke. The SAED pattern shows diffuse carbon rings consistent with the EDS spectrum showing only C. Particle sizes range from <math><50\text{ nm}</math> to \text{TiO}_2 (rutile) nanoparticles. Oxygen signal is absent in EDS spectrum for particulates collected on carbon/formvar-coated Cu 100 mesh grid. Note R in EDS spectra indicates relative intensity. This applies to all EDS spectra following.

Figure 2. Mixture of ambient air PM. (a) carbonaceous particulate with nanocrystal inclusions in surrounding wall structure indicated by diffraction spots at arrows. (b) carbonaceous (graphitic) layered aggregate. Layer thickness $\sim 10\text{ nm}$ as shown. SAED pattern insert shows diffuse carbon rings. (c) microcrystalline layered aggregate. (d) Systematic, overlapping crystal aggregate which appears to be organic/carbonaceous matter. (e) Complex silica (SiO_2) aggregate of very tiny ($<1\text{ nm}$) nanocrystals. (f) Carbonaceous aggregate. SAED pattern shows only diffuse carbon rings.

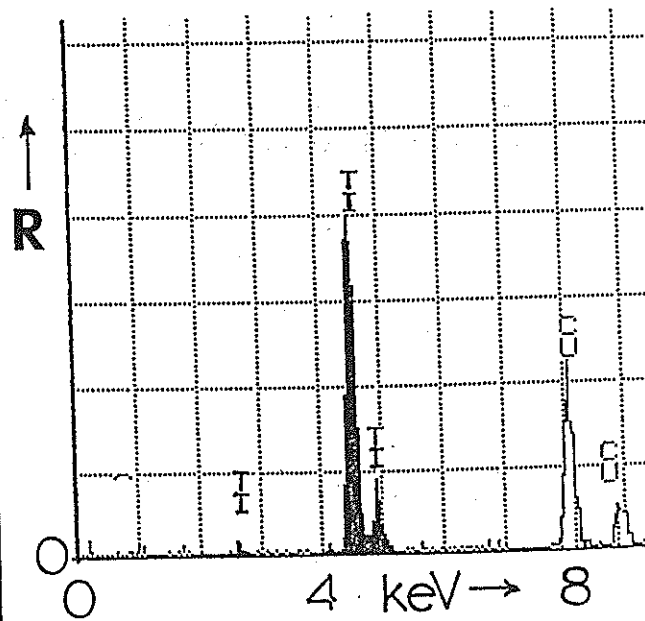
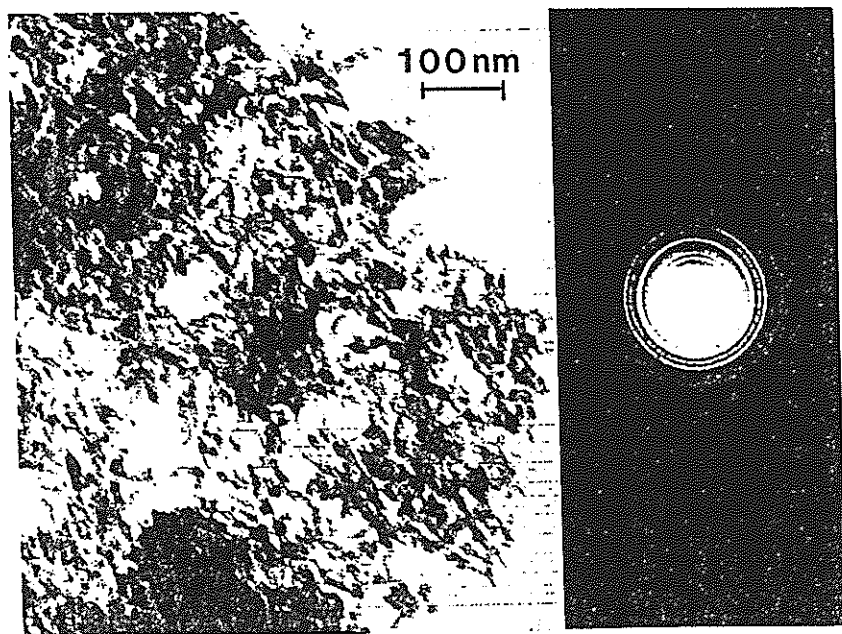
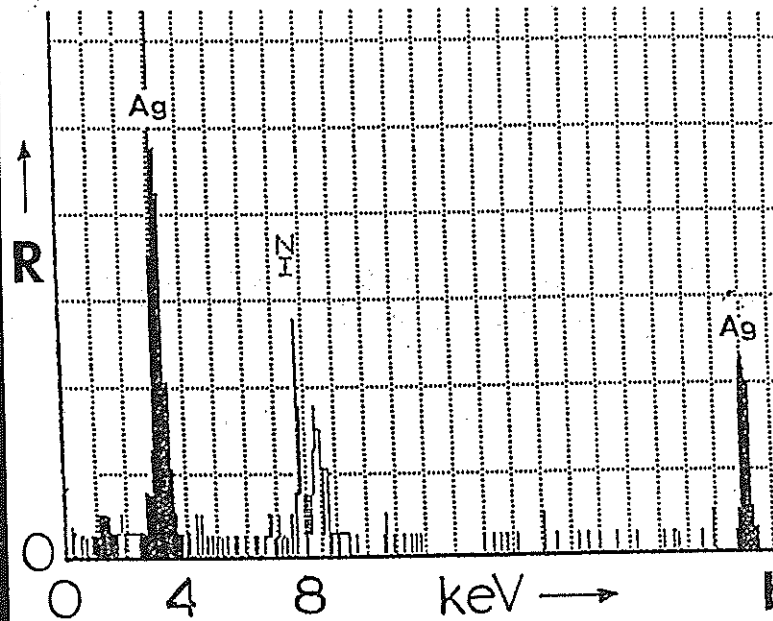
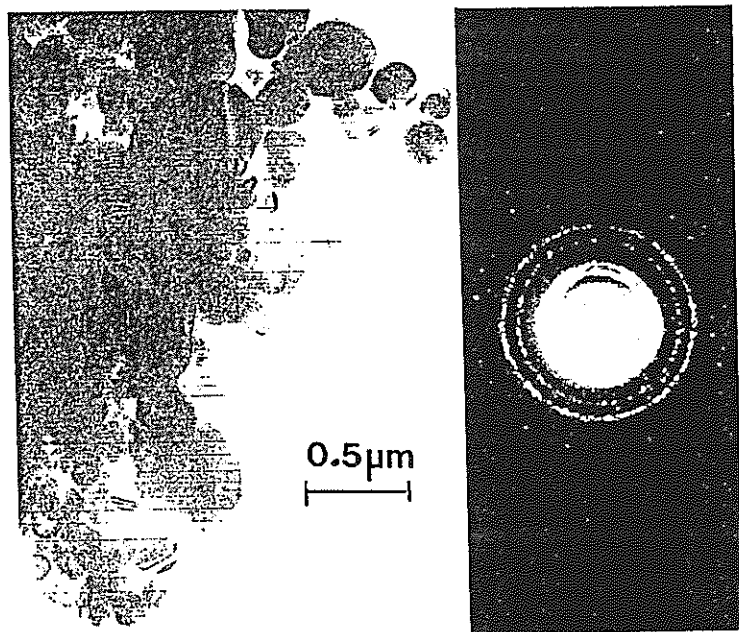
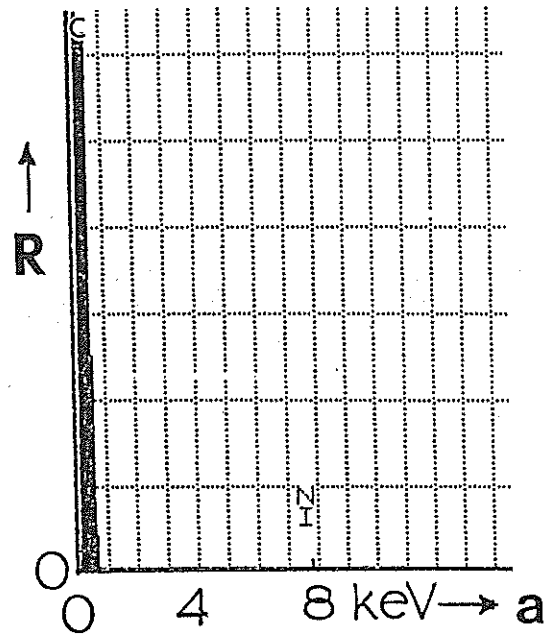
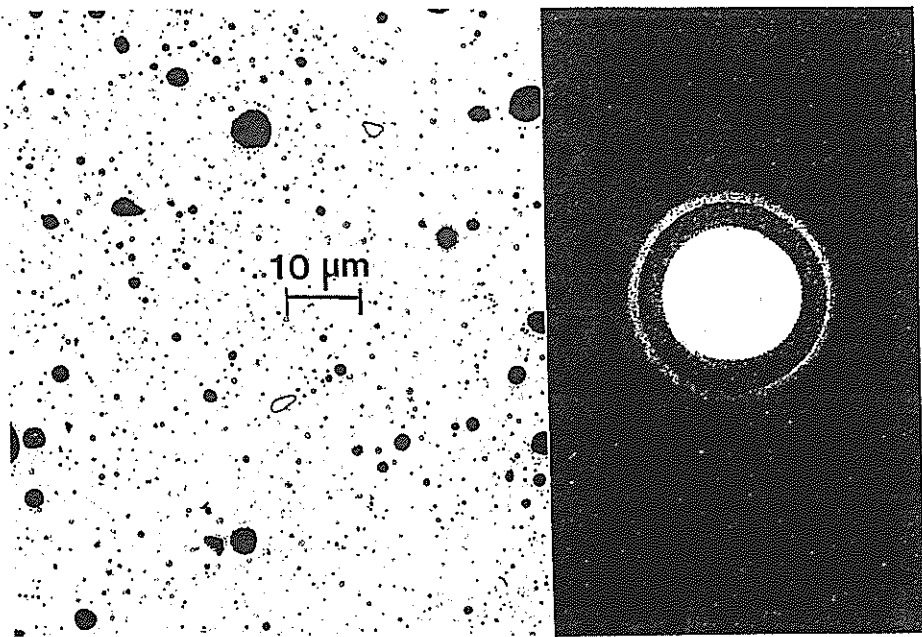
Figure 3. Brake-shop airborne PM collection examples. (a) Graphitic carbon multi-layer (arrow) particulate. SAED pattern insert shows diffuse carbon rings. (b) Complex nanocrystalline aggregate PM. (c) TEM, SAED pattern, EDS sequence for TiO_2 (rutile) crystal cluster. O $K\alpha$ peak overlaps Ti $L\alpha$ peak in EDS spectrum. (d) TEM, EDS spectrum with SAED pattern insert showing large Ca-rich aggregate composed of thousands of nanocrystals. Note small Sn component. Ni peak is the 100 mesh grid.

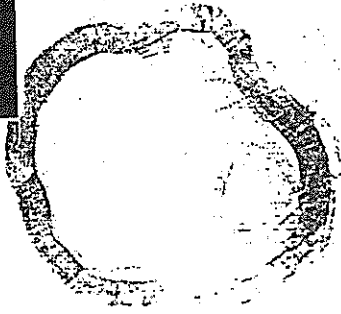
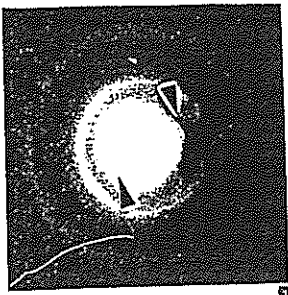
Figure 4. Diesel exhaust particulates. (a) TEM image of DPM aggregate in diesel truck exhaust stream, SAED pattern, and corresponding EDS-carbon peak. The SAED pattern shows diffuse C rings. (b) and (c) show diesel truck exhaust aggregates. (d) TEM, SAED pattern and EDS sequence for a carbonaceous aggregate collected in the air at a diesel truck area. Trace of S is observed in the EDS spectrum along with prominent C peak.

Figure 5. Examples of carbonaceous/inorganic nanocrystalline PM collected along with carbonaceous DPM. (a) TEM image, SAED pattern insert, EDS spectrum sequence for PM mixture. (b) TEM image, SAED pattern insert, EDS spectrum sequence for titania cluster. Note diffraction contrast fringes prominent for crystal marked by arrow.

Figure 6. Particulates collected in outdoor El Paso air locations. (a) TEM image, SAED pattern, and EDS sequence for carbonaceous wood burn aggregate. (b) TEM image, SAED pattern, and EDS sequence for complex inorganic (crystalline)-carbonaceous aggregate. Inorganic crystals are Al-Cu rich. SAED pattern insert shows prominent diffuse C rings superimposed on crystal (spot) diffraction patterns. C and O peaks in EDS spectrum are under-represented in the signal. (c) TEM image, SAED pattern, and EDS sequence for Cu-rich polycrystalline aggregate collected near a copper smelter-site.

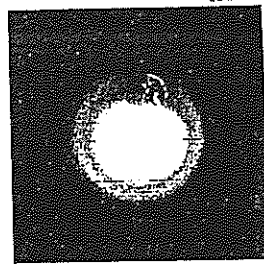
Figure 7. Jet engine exhaust particulates. (a) Complex, nanocrystalline aggregate (W, Ag, Cu components) intermixed with carbonaceous matter as illustrated in the TEM image, EDS/SAED pattern insert sequence. (b) Carbonaceous-rich, Si-containing nanocrystal aggregate collected on 100 mesh Ni grid with carbon/formvar substrate. TEM image, EDS/SAED pattern insert sequence.



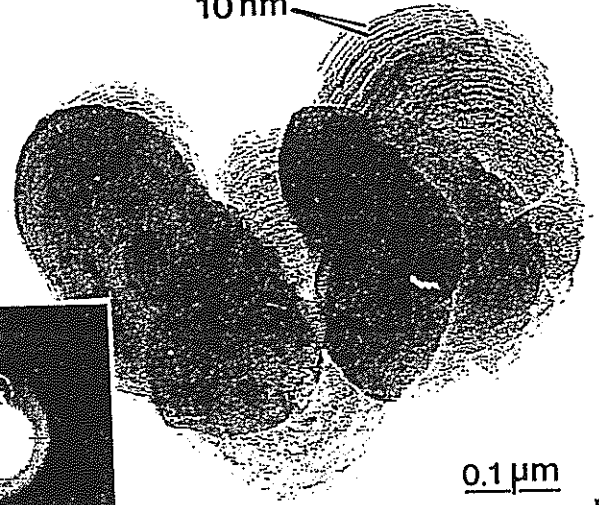


50nm

a

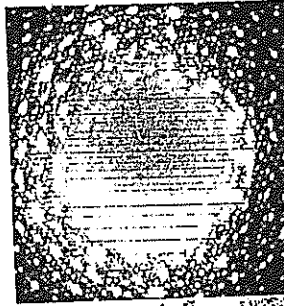


10nm



0.1 μm

b



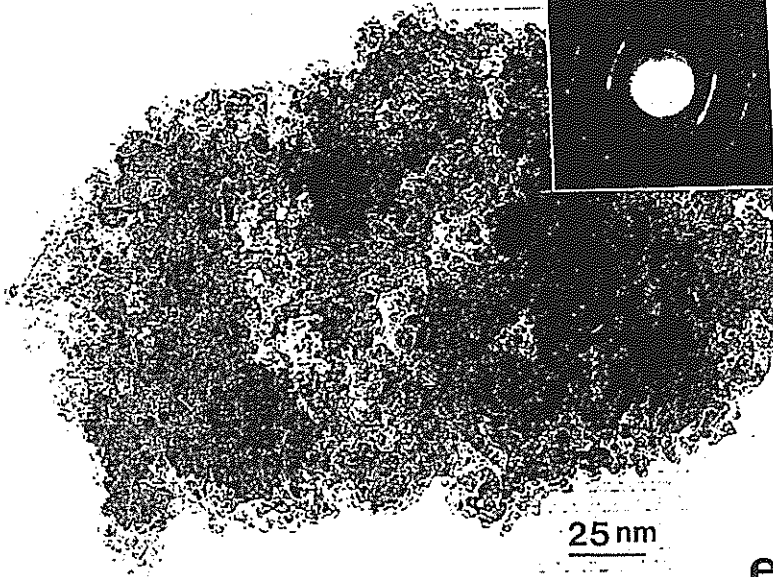
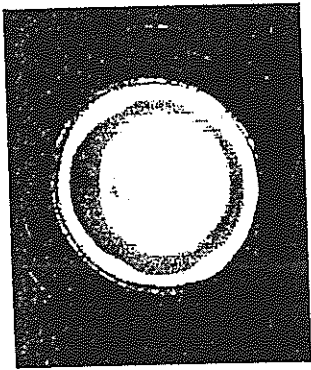
0.1 μm

c



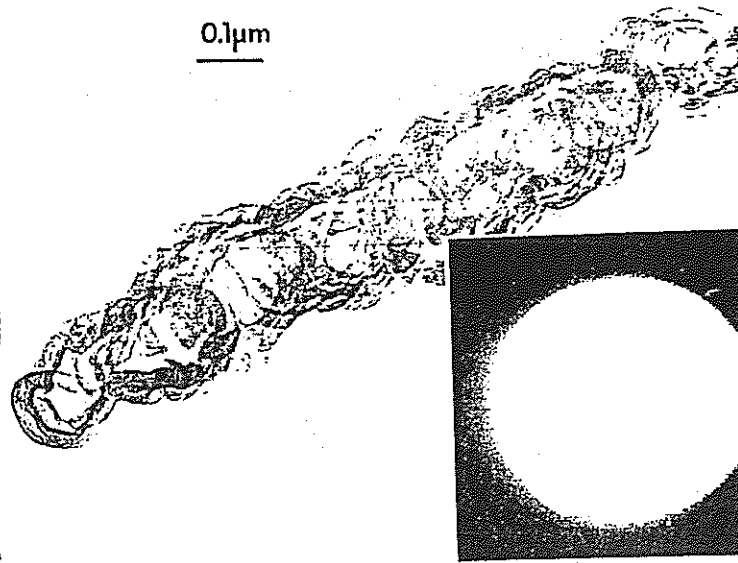
0.3 μm

c



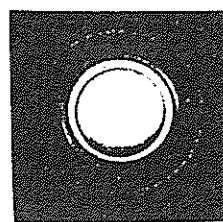
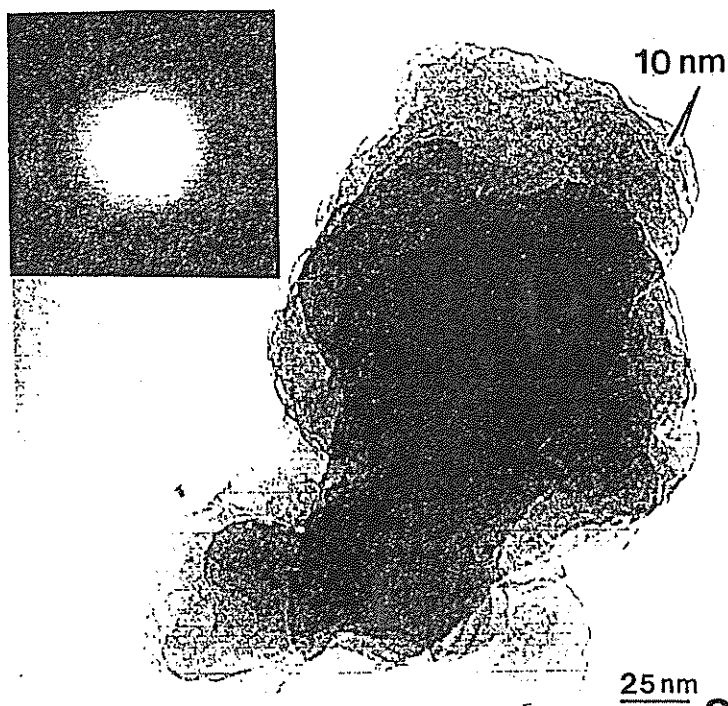
25 nm

e



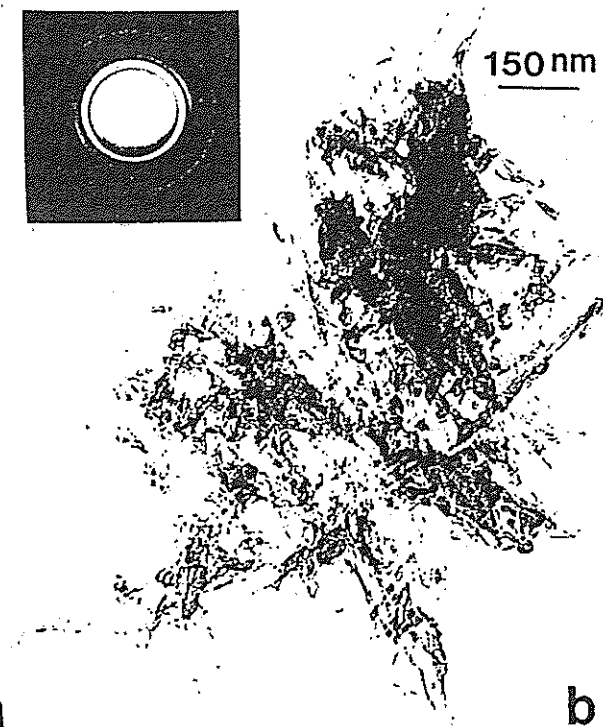
0.1 μm

Fig 2

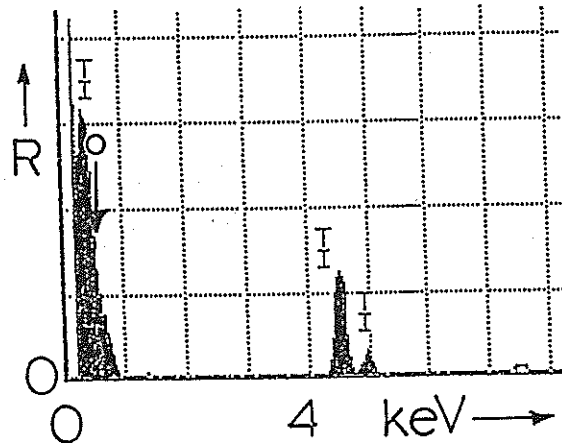
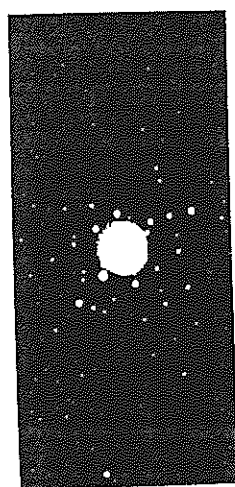


25 nm

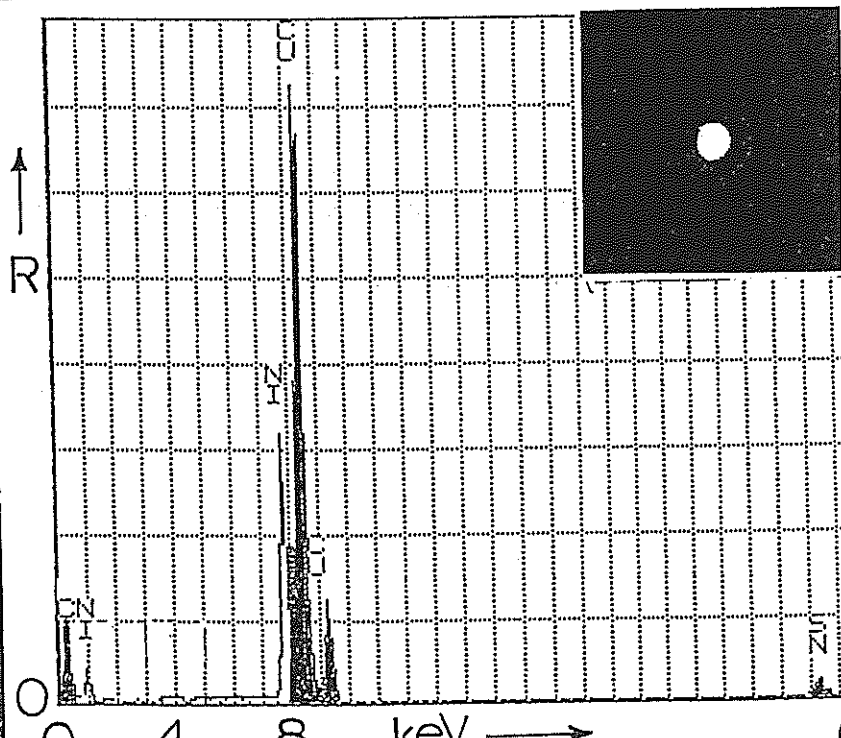
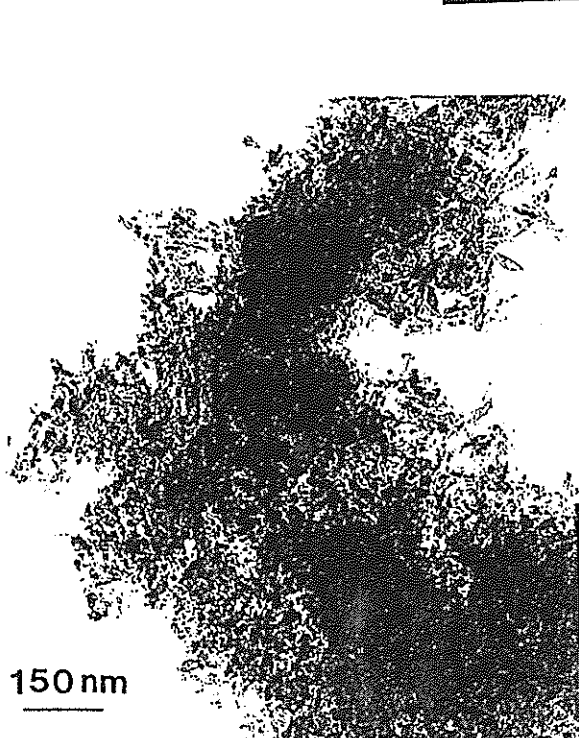
a



b



c



d

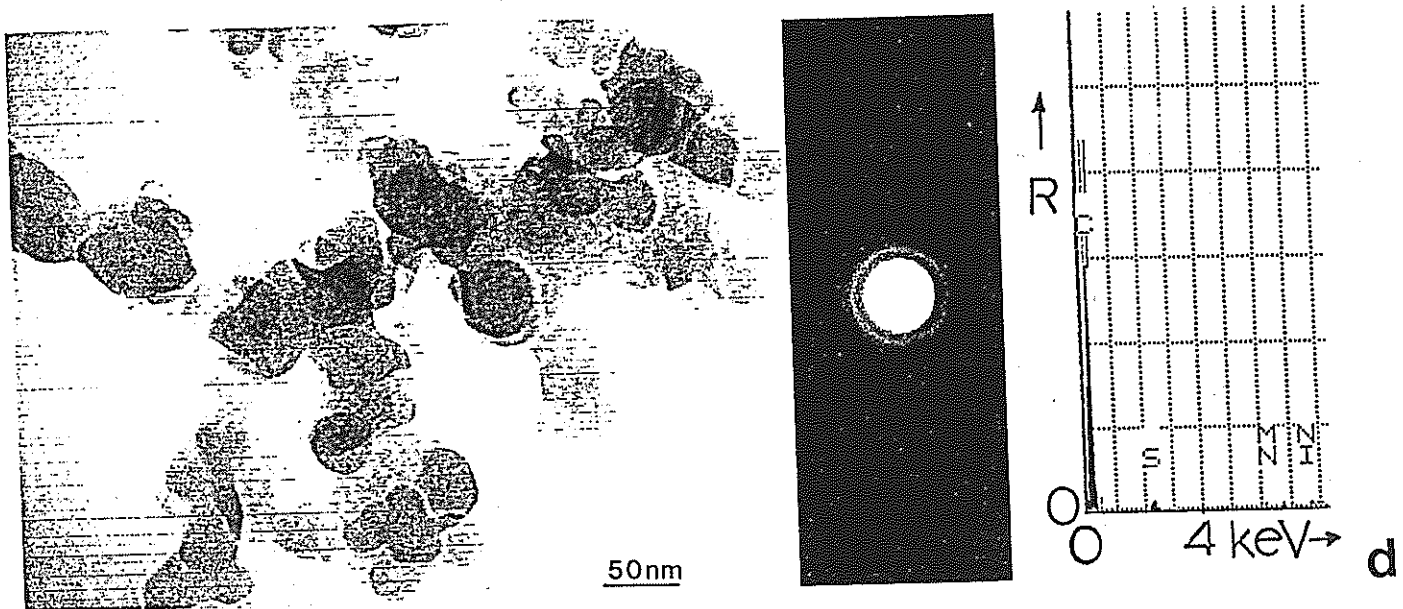
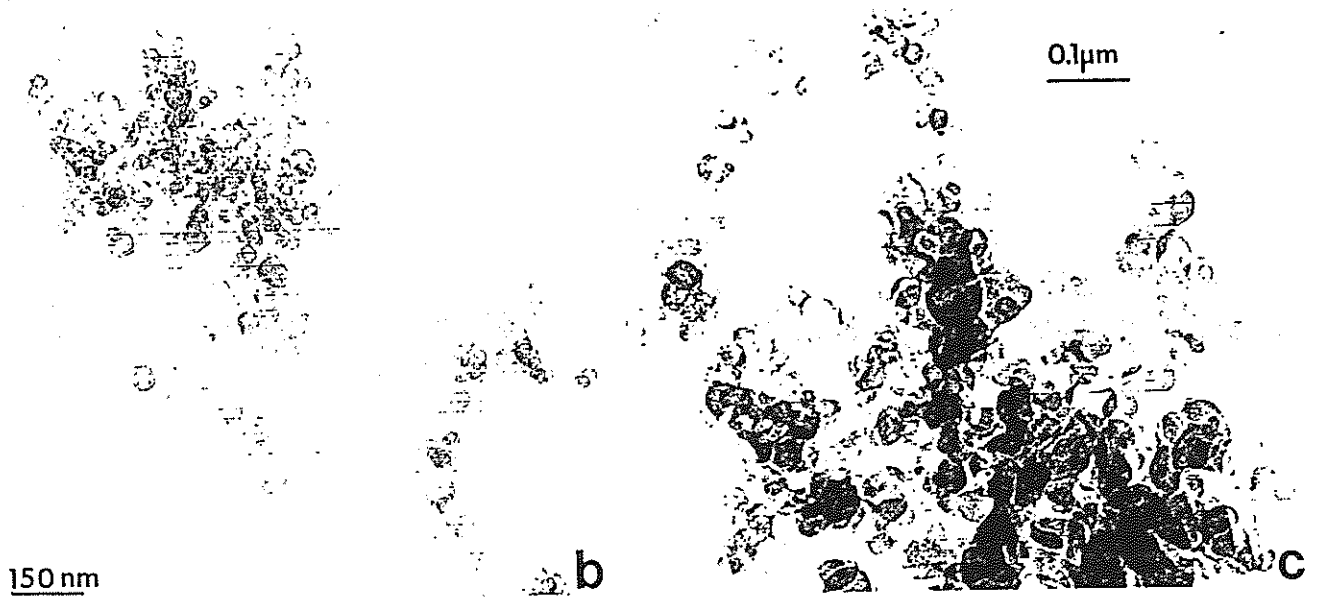
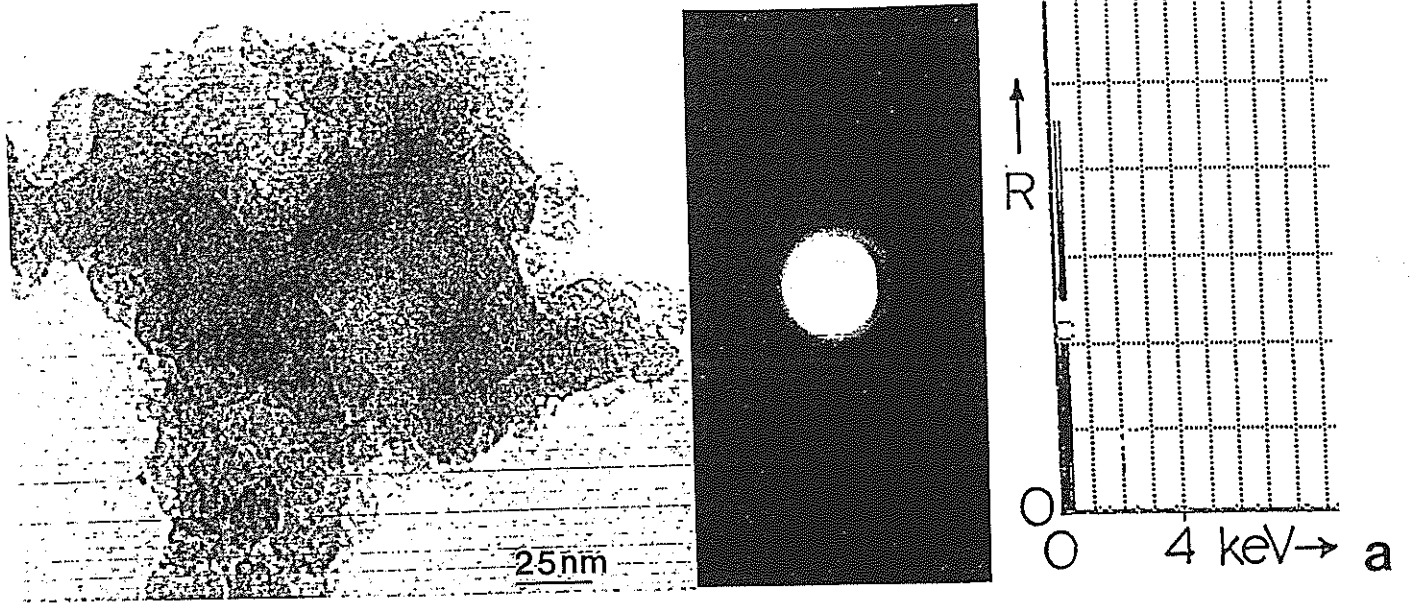
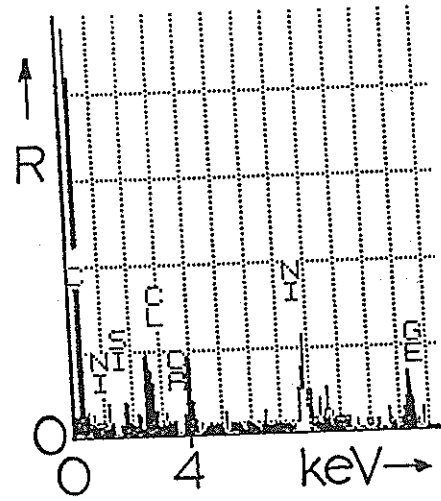
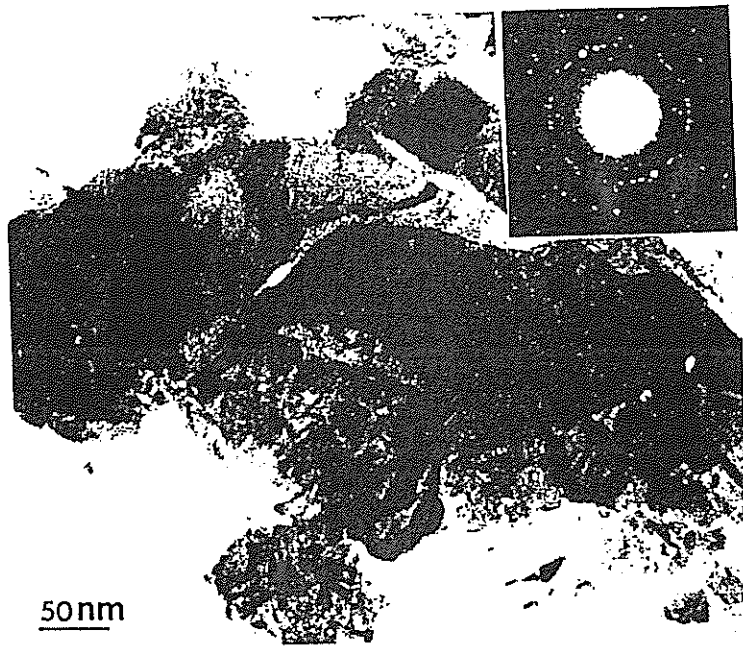
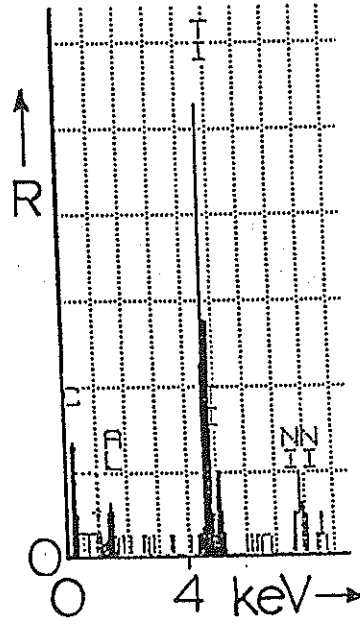
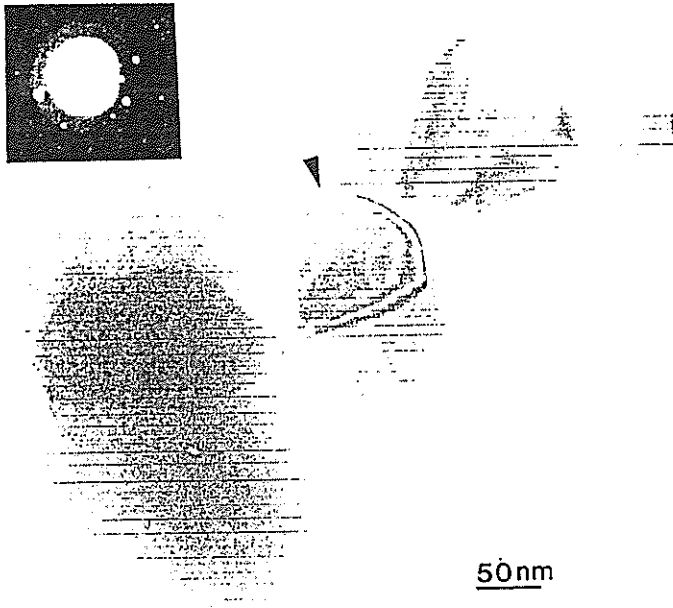


FIG. 4 Murr & Gray



a



b

FIG. 5 Murr & Bong

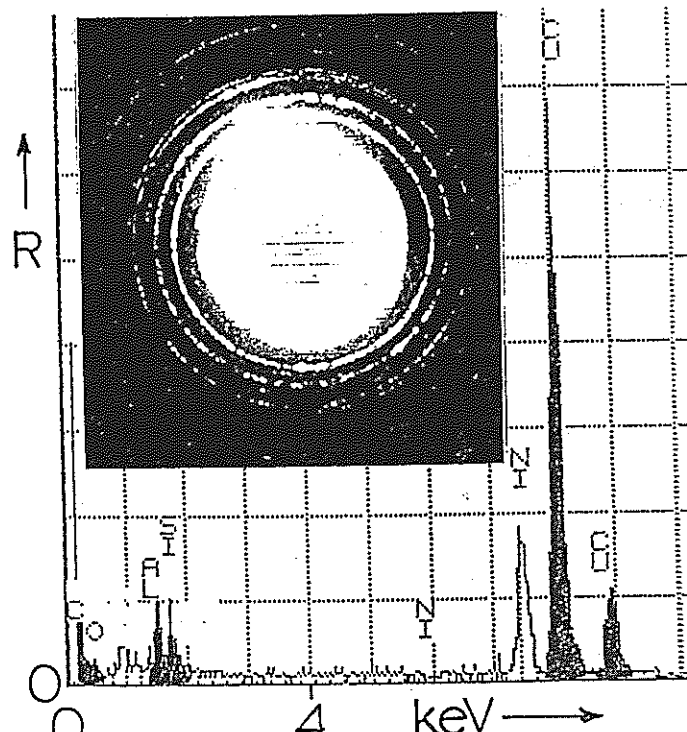
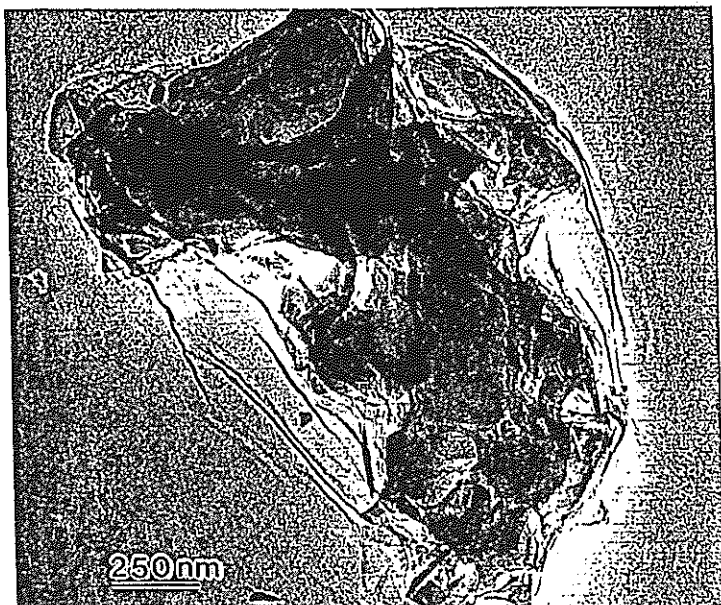
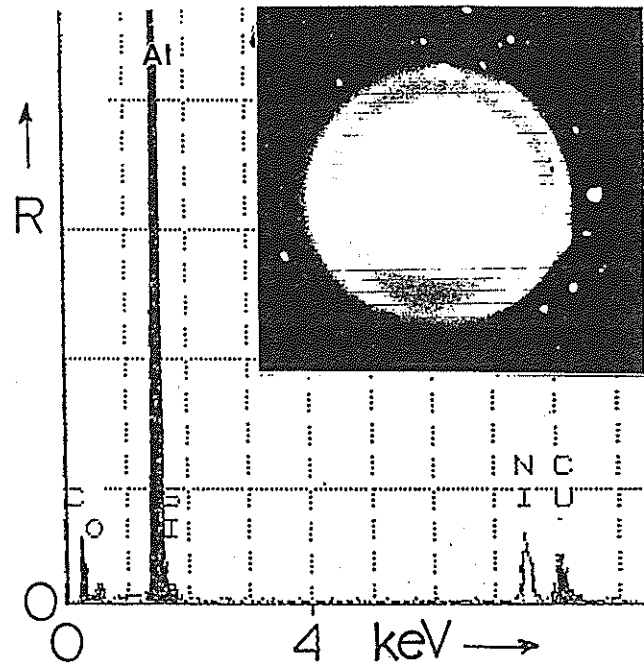
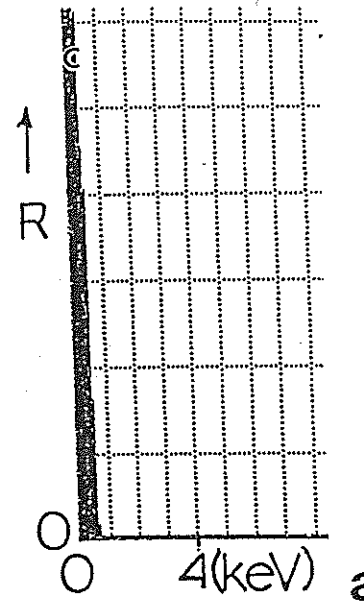
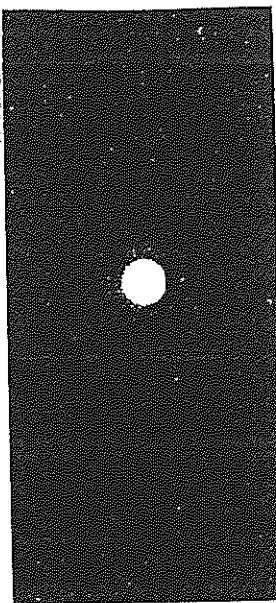
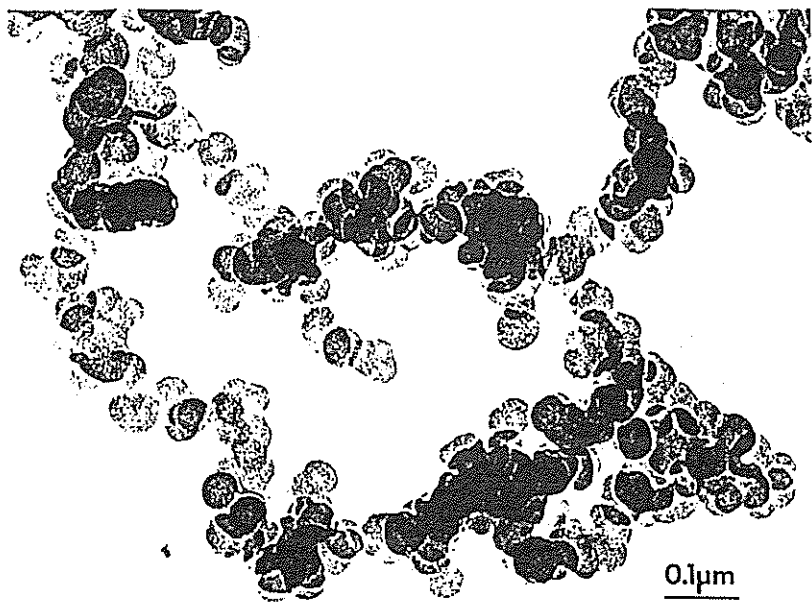


FIG. 6

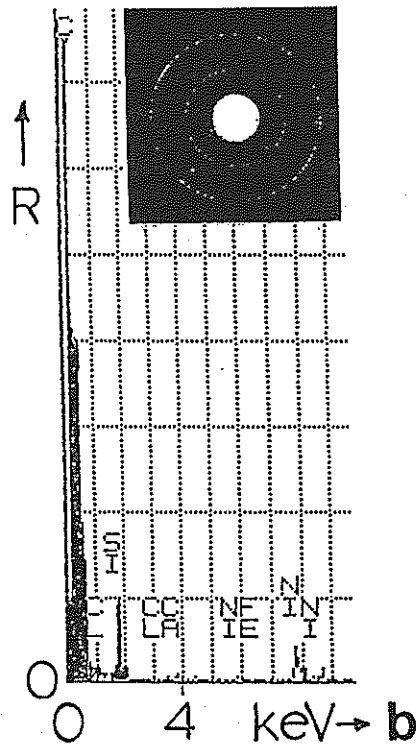
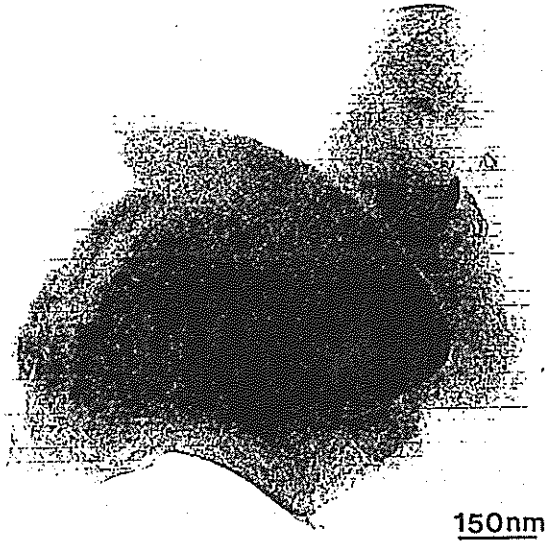
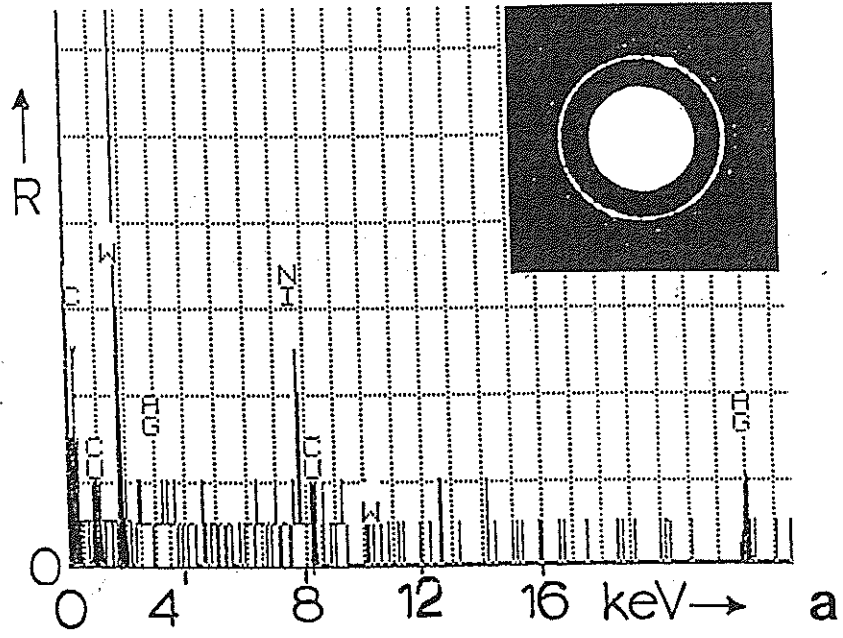
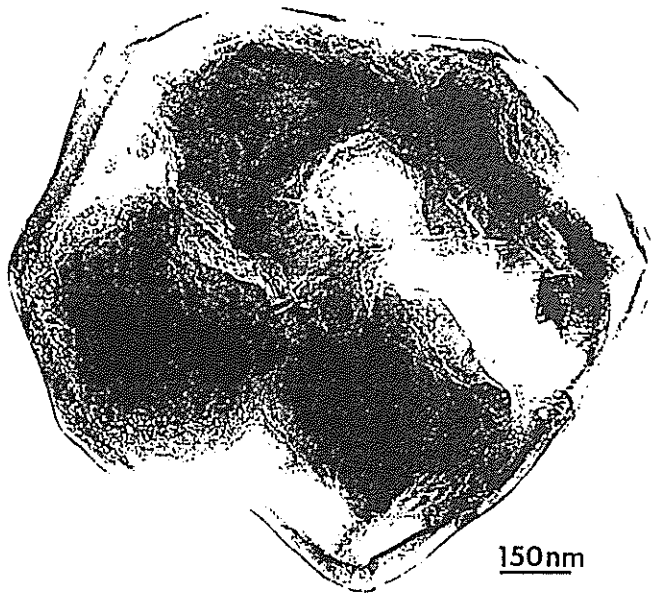


FIG. 7 Murr & Banj

